

Nb and Ta Adducts: Connecting d^0 Metal Chlorides and Phosphorus Sulfide Cages

Diana Hoppe,^[a] Dominik Schemmel,^[b] Martin Schütz,^{*[b]} and Arno Pfitzner^{*[a]}

Abstract: Phosphorus sulfide cages α -P₄S₄, α -P₄S₅, β -P₄S₅, and β -P₄S₆ and transition-metal chlorides TaCl₅ and NbCl₅ form molecular adducts in CS₂/*n*-hexane. The crystal structures of the adducts (TaCl₅)(α -P₄S₄), (TaCl₅)(α -P₄S₅), (TaCl₅)(β -P₄S₅), (NbCl₅)(β -P₄S₅), and (TaCl₅)(β -P₄S₆) are reported and

their conformation and energetic stability are discussed on the basis of ab initio electronic structure calculations.

Furthermore bond lengths of coordinated and noncoordinated phosphorus sulfide cages obtained from experiment and theory are compared, emphasizing the changes within the cages that emerge upon coordination.

Keywords: ab initio calculations · molecular adducts · niobium · phosphorus · sulfur · tantalum

Introduction

Neutral molecules, such as Ph₃P or CO, are frequently used as ligands for metal complexes. Among the more uncommon species of this group are cage-like nonmetal molecules that can act as electron pair donors towards the metal. This research topic has been of wide interest over recent years.^[1] With restriction to transition-metal halides such as TiX₄ or NbX₅ (X = halogen), adducts such as (NbCl₅)₂(β -P₄S₄) and (NbCl₅)(P₄Se₃)^[2] or (TiX₄)₂(S₄N₄)₂ (X = Cl, Br, I)^[1b,e,h] were reported. We are now interested whether other cages, especially phosphorus chalcogenide cages, can be used for such purposes.

Screening with different phosphorus sulfides was carried out. They show a broader structural variety than the selenides and are easier to prepare and handle, since phosphorus selenides tend to glass formation and are much less soluble in any solvent.

In addition to the co-crystals (M₂Cl₁₀)(P₄S₁₀)₂^[3] and the (MCl₅)₂(β -P₄Ch₄) adducts^[4] isotypic with (NbCl₅)₂(β -P₄S₄)^[2] (M = Nb, Ta; Ch = S, Se), new adduct compounds of different phosphorus sulfide cages could now be obtained: (TaCl₅)(α -P₄S₄), (TaCl₅)(α -P₄S₅), (TaCl₅)(β -P₄S₅), (NbCl₅)(β -P₄S₅), and (TaCl₅)(β -P₄S₆).

To understand the nature of the binding between metal center and cage, electronic structure calculations were performed employing density functional theory (DFT) as well as ab initio wavefunction-based methods. DFT yields exceedingly low binding energies and distances considerably too long for the coordinative bond between metal center and cage (in comparison to the experimental results). This result suggests that a major fraction of the binding energy may come from long-range van der Waals dispersion, which is not described at all by DFT in conjunction with common functionals. Therefore, the individual adducts were studied also at the level of Møller Plesset perturbation theory of second order (MP2), the computationally cheapest method capturing dynamical correlation effects (and thus van der Waals dispersion). In the present study, we employed the local MP2 (LMP2) method,^[17] which apart from higher computational efficiency, also offers some additional benefits over the canonical MP2 method.^[21] Of course, MP2 can only be applied if near degeneracy effects are absent. Indeed, the adducts investigated in the present study are not multirefer-

[a] Dr. D. Hoppe, Prof. Dr. A. Pfitzner
Institut für Anorganische Chemie
Universität Regensburg
93040 Regensburg (Germany)
Fax: (+49)941-943-814551
E-mail: arno.pfitzner@chemie.uni-regensburg.de

[b] D. Schemmel, Prof. Dr. M. Schütz
Institut für Physikalische und Theoretische Chemie
Universität Regensburg
93040 Regensburg (Germany)
Fax: (+49)941-943-4719
E-mail: martin.schuetz@chemie.uni-regensburg.de

Supporting information for this article is available on the WWW under <http://dx.doi.org/10.1002/chem.200900370>. It contains tables of interaction, relaxation, and binding energies of the structures and their coordination alternatives and interaction energies; calculated with the X = T basis set at Hartree–Fock local (with normal and by one-bond extended domains) and canonical MP2 levels of theory.

ence cases, as we could verify by initially performing complete active space self-consistent field (CASSCF) test calculations. Hence, LMP2 appears to be a suitable method for the present case.

Results and Discussion

Constitution and packing: Crystal-structure analysis showed that the title compounds are small adduct molecules consisting of one TaCl_5 or NbCl_5 unit linked with a phosphorus sulfide cage (Figures 1–4). The constitution of the respective

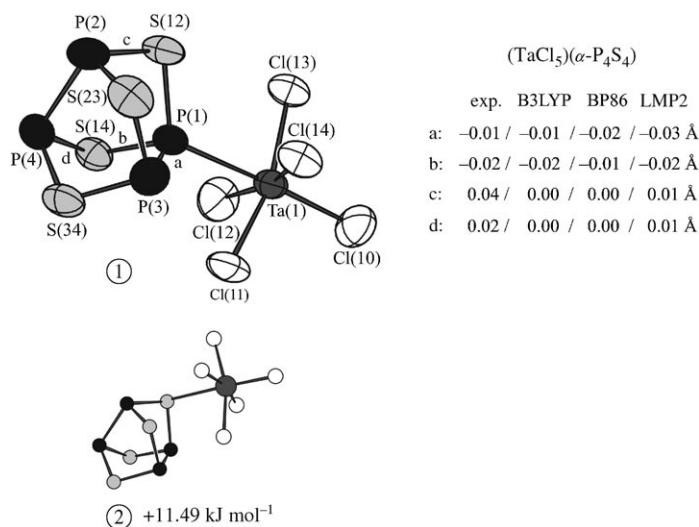


Figure 1. Experimental and calculated structures of $(\text{TaCl}_5)(\alpha\text{-P}_4\text{S}_4)$. Phosphorus: black, sulfur: light gray, tantalum: dark gray, chlorine: white. Left: Crystal structure; ellipsoids enclose 70% probability for atomic displacement. Right: The four largest changes (labeled a, b, c, d) in bond lengths from experimental results and calculations with DFT (using B3LYP and BP86 xc functional, aug-cc-pVTZ AO basis set) and LMP2 (by one-nearest-neighbor extended domains, aug-cc-pVDZ AO basis set) level of theory. Bottom: coordination alternatives with relative energies relative to coordination modes found. See Table 2.

phosphorus sulfide part does not change upon coordination. In contrast to the starting materials, tantalum and niobium pentachloride are monomeric in all analyzed adducts. A distorted octahedron was found as the coordination sphere around the metal atom for each adduct. The coordinative bond towards the metal atoms is formed by a terminal sulfur atom, if present, or otherwise by a phosphorus atom of the cages.

The dumbbell-shaped molecules are arranged in distorted hexagonal layers with the layers oriented parallel to the crystallographic (001) planes in all cases (Figure 5).

In $(\text{TaCl}_5)(\alpha\text{-P}_4\text{S}_4)$, one of the four equivalent phosphorus atoms of the D_{2d} -symmetrical $\alpha\text{-P}_4\text{S}_4$ molecule is connected to one metal chloride unit. The C_s symmetry of the resulting adduct is almost preserved in the crystal structure.

In the closely related adducts $(\text{NbCl}_5)(\beta\text{-P}_4\text{S}_5)$ and $(\text{TaCl}_5)(\beta\text{-P}_4\text{S}_5)$, one phosphorus atom of the remaining P_2

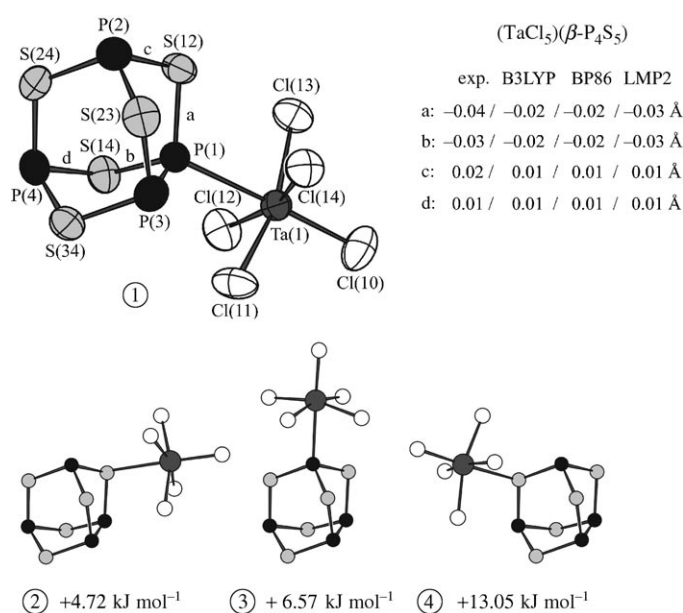


Figure 2. Experimental and calculated structures of $(\text{TaCl}_5)(\beta\text{-P}_4\text{S}_5)$; see legend of Figure 1.

dumbbell in the C_{2v} -symmetrical $\beta\text{-P}_4\text{S}_5$ cage is bound to the metal chloride unit. The deviation of the adduct molecule from C_s symmetry is a bit larger than that in $\alpha\text{-P}_4\text{S}_4$ -containing molecules. As the two $\beta\text{-P}_4\text{S}_5$ -containing adducts are similar, only the one with TaCl_5 will be referred to further.

In $(\text{TaCl}_5)(\alpha\text{-P}_4\text{S}_5)$ and $(\text{TaCl}_5)(\beta\text{-P}_4\text{S}_6)$, the terminal sulfur atoms of the cages form coordinative bonds to the metal atoms. Since the free $\alpha\text{-P}_4\text{S}_5$ cage is entirely unsymmetrical, the adduct molecules of $(\text{TaCl}_5)(\alpha\text{-P}_4\text{S}_5)$ are unsymmetrical as well. $\beta\text{-P}_4\text{S}_6$, in contrast, exhibits C_s symmetry. However, the adduct molecules $(\text{TaCl}_5)(\beta\text{-P}_4\text{S}_6)$ also have only C_1 symmetry. The two compounds crystallize with very similar packing of the molecules. The projections of the crystal structures along the [100] direction are given in Figure 5.

Conformation: Nonperiodic ab initio electronic-structure calculations were performed to assess the strength of the interaction between TaCl_5 and the individual cages and to study alternative conformers not observed experimentally. The geometry optimizations of the individual adduct molecules yielded structural parameters that are reasonably close to those observed in the crystal structures. Therefore, the orientations of the four equatorial chlorine atoms of the MCl_5 groups (anticipated to rotate almost freely), and the orientations of the whole MCl_5 units relative to the individual cages (for molecules with a terminal sulfur atom at the cages) observed experimentally are not primarily related to crystal formation but a property of the individual adduct molecules themselves.

Nevertheless, there are small deviations: In $(\text{TaCl}_5)(\alpha\text{-P}_4\text{S}_4)$ and $(\text{TaCl}_5)(\beta\text{-P}_4\text{S}_5)$, the TaCl_5 unit is turned out of the “ideal” position for C_s symmetry by up to 10°, which cannot be considered as being the energetic minimum of the single

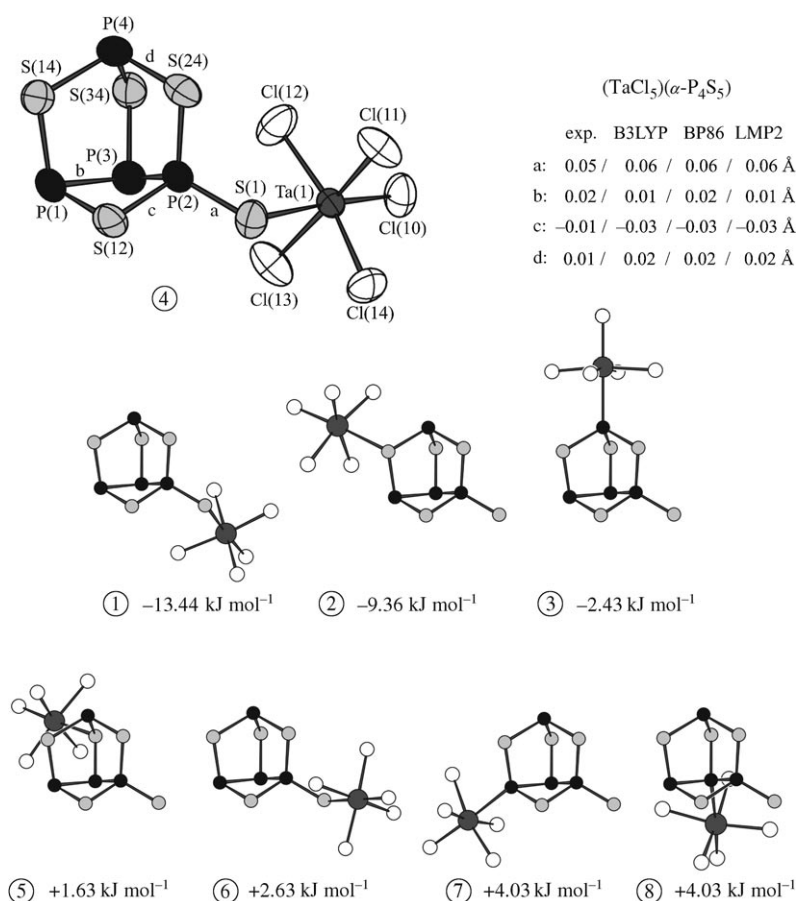


Figure 3. Experimental and calculated structures of (TaCl₅)(α -P₄S₅); see legend of Figure 1.

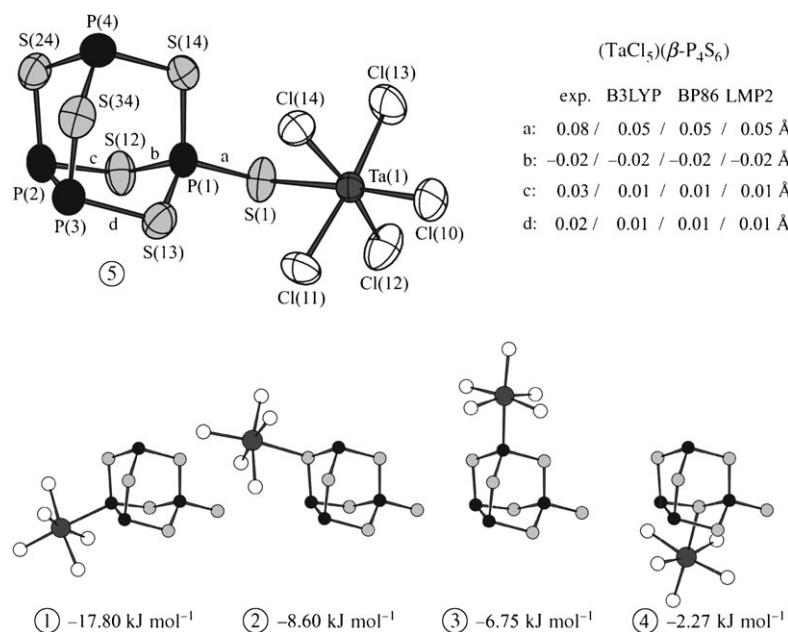


Figure 4. Experimental and calculated structures of (TaCl₅)(β -P₄S₆); see legend of Figure 1.

molecule and which therefore has to be attributed to the influence of intermolecular forces or packing of molecules in the crystal.

In the two adduct molecules with a terminal sulfur atom connected to the metal center, the TaCl₅ units possess greater flexibility because of the additional P–S_{terminal} rotation axis. Closer examination of the molecular conformation of (TaCl₅)(α -P₄S₅) and (TaCl₅)(β -P₄S₆) reveals that stabilizing intramolecular interactions may force the metal chloride units to arrange as observed. The closest chlorine atoms reach more or less into a cavity of the cage—a five-membered ring of phosphorus and sulfur of the α -P₄S₅ cage and a six-membered ring of the β -P₄S₆ cage. Thus, comparatively short distances between the nonbonded atoms S(1) and Cl(14) in α -P₄S₅ of 3.19 Å (exptl)/3.20 Å (calcd) and between S(1) and Cl(12) in β -P₄S₆ of 3.16 Å (exptl)/3.19 Å (calcd) result. Rotation about the P–S_{terminal} axis leads to conformers that display energetic minima as well (see below).

As already stated, the coordination octahedra of the metal atoms formed by chlorine and phosphorus or sulfur atoms are distorted. The angles (Cl_{equatorial}–Ta–Cl_{axial}) are enlarged, which shifts the equatorial chlorine atoms towards the phosphorus or sulfur atoms, so the metal atoms lie about 0.2 to 0.4 Å from the Cl_{equatorial} plane. In addition, the P–Ta–Cl_{axial} or S–Ta–Cl_{axial} axis bends. The corresponding bond angles are 173.7° (exptl)/175.0° (calcd) for the α -P₄S₄ adduct, 175.1° (exptl)/174.9° (calcd) for the β -P₄S₅ adduct with Ta, 175.8° (exptl)/176.3° (calcd) for the α -P₄S₅ adduct, and 173.6° (exptl)/173.5° (calcd) for the β -P₄S₆ adduct. The distortion can be attributed to a second-order

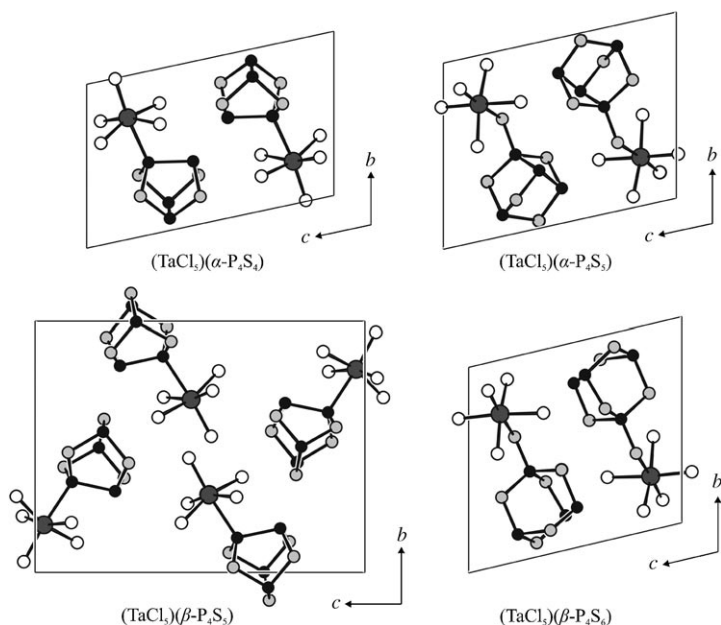


Figure 5. Projection of the crystal structures of $(\text{TaCl}_5)(\alpha\text{-P}_4\text{S}_4)$, $(\text{TaCl}_5)(\alpha\text{-P}_4\text{S}_5)$, $(\text{TaCl}_5)(\beta\text{-P}_4\text{S}_5)$, and $(\text{TaCl}_5)(\beta\text{-P}_4\text{S}_6)$ in the [100] direction. Phosphorus: black, sulfur: light gray, tantalum: dark gray, chlorine: white.

Jahn–Teller effect^[37] usually observed, for example, in octahedral complexes of d^0 transition metals (e.g. $\text{Na}[\text{TaCl}_6]$).^[38]

Bond lengths: The experimentally obtained and the calculated distances $d(\text{P–Ta})$ (or $d(\text{S–Ta})$), and the different bond lengths within the individual cages of the four adducts are compiled in Table 1. Evidently, the calculated LMP2 values for the distances $d(\text{P–Ta})$ of the isolated complexes are in good agreement with the values measured in the crystal. They deviate by 0.017 and 0.003 Å from the experimental values for $(\text{TaCl}_5)(\alpha\text{-P}_4\text{S}_4)$ and $(\text{TaCl}_5)(\beta\text{-P}_4\text{S}_5)$, respectively. For DFT, the agreement is much worse; for example, for the B3-LYP case, the corresponding deviations amount to 0.138 and 0.133 Å.

For the distances $d(\text{S–Ta})$ in the adducts in which the free terminal sulfur atoms act as the donors of the cages, the deviations between the calculated LMP2 values and the experimental values measured in the crystal increase to 0.07 Å for $(\text{TaCl}_5)(\alpha\text{-P}_4\text{S}_5)$ and to 0.096 Å for $(\text{TaCl}_5)(\beta\text{-P}_4\text{S}_6)$. Again, the discrepancies for the corresponding B3-LYP results are significantly larger, amounting to 0.178 and to 0.21 Å, respectively. Since the latter complexes are more flexible (see above), the influence of crystal packing on their structural parameters is expected to be larger than for adducts with a direct linkage of Ta to a P atom of the cage. Hence, the bigger discrepancies between calculated and measured values for the distances $d(\text{S–Ta})$ are not surprising.

The bad performance of DFT in comparison with LMP2 indicates that van der Waals dispersion (absent in DFT calculations employing the usual xc functionals) plays a crucial role in the binding between TaCl_5 and the individual cages. Furthermore, if van der Waals dispersion contributes sub-

stantially to the binding energy, then the LMP2 results are likely to improve further when the AO basis set is extended and the large core pseudopotential for tantalum is substituted by a small core pseudopotential (presently not available). The importance of van der Waals dispersion in the binding of these adducts will be discussed further in the next section.

Coordination causes certain bonds within the individual cages to contract or elongate, as is evident from experimental as well as theoretical data compiled in Figures 1–4 and Table 1. As known from other adduct molecules such as $(\text{SbCl}_5)(\text{S}_4\text{N}_4)$ ^[39] or $(\text{SbCl}_5)(\text{S}_8\text{O})$,^[40] the formation of the coordinative bond between Lewis acid (electron-pair acceptor) and Lewis base (electron-pair donor, phosphorus sulfide in this case) not only weakens the adjacent bond but also alters the bond lengths throughout the whole cage molecule (Figure 6). In $(\text{SbCl}_5)(\text{S}_4\text{N}_4)$, this even leads to cleavage of the S–S bonds: the S_4N_4 molecule connected to SbCl_5 is merely annular.^[41]

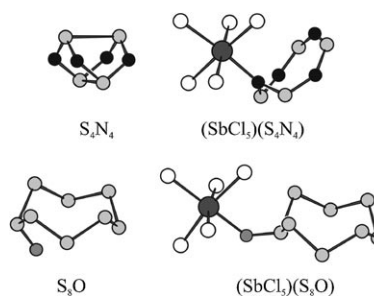


Figure 6. Molecules S_4N_4 ,^[41] S_8 ,^[42] and adducts $(\text{SbCl}_5)(\text{S}_4\text{N}_4)$ ^[39] and $(\text{SbCl}_5)(\text{S}_8\text{O})$.^[40] Antimony: dark gray, chlorine: white, sulfur: light gray, nitrogen: black, oxygen: medium gray.

For the adducts presented herein, it is notable that especially the bond between phosphorus and the terminal sulfur atoms, if present, lengthens considerably upon coordination, as do the second nearest bonds within the cages (this situation holds also for adducts linked through phosphorus), whereas the bonds in between are shortened slightly. In Figures 1–4, bonds that show the strongest alterations upon coordination of the metal chloride units are marked with a, b, c, and d. The scheme of alternate elongation and contraction of bonds is disturbed by the shape of the cages, being composed of concatenated rings of atoms. In $(\text{SbCl}_5)(\text{S}_8\text{O})$, the analogous sequence of bond elongation and shortening relative to the noncoordinated S_8O can be followed more explicitly because of the ring shape of the sulfur oxide.^[40,42]

The local MP2 geometries mostly confirm these subtle changes of bond lengths (cf. Figures 1–4 and Table 1). For $(\text{TaCl}_5)(\alpha\text{-P}_4\text{S}_4)$, bonds of the phosphorus atom P(4) as well as the P(2)–S(12) bond are found to be significantly elongated, the P(1)–S(14) bond in contrast is shortened. In $(\text{TaCl}_5)(\beta\text{-P}_4\text{S}_5)$, bonds of the phosphorus atom P(1), which is directly connected to tantalum, is shortened, the adjacent

Table 1. Bond lengths [Å] in coordinated and noncoordinated cages.

Bond	Exptl ^[a]	$\alpha\text{-P}_4\text{S}_4$			$(\text{TaCl}_5)(\alpha\text{-P}_4\text{S}_4)$				
		B3LYP	BP86	LMP2	Exptl	B3LYP	BP86	LMP2	
P(1)	–P(3)	2.3530(8)	2.410	2.420	2.403	2.340(6)	2.397	2.404	2.375
	–S(12)	2.1117(7)	2.139	2.141	2.146	2.104(5)	2.124	2.129	2.123
	–S(14)	2.1095(7)	2.139	2.141	2.146	2.086(6)	2.124	2.129	2.123
P(2)	–P(4)	2.3530(8)	2.409	2.419	2.403	2.379(6)	2.416	2.429	2.415
	–S(12)	2.1068(8)	2.139	2.141	2.146	2.148(6)	2.141	2.142	2.155
	–S(23)	2.1145(7)	2.139	2.141	2.146	2.117(9)	2.141	2.143	2.149
P(3)	–S(23)	2.1145(7)	2.139	2.141	2.146	2.134(7)	2.137	2.140	2.148
	–S(34)	2.1068(8)	2.139	2.141	2.146	2.089(7)	2.137	2.140	2.148
P(4)	–S(14)	2.1095(7)	2.139	2.142	2.146	2.131(5)	2.141	2.142	2.155
	–S(34)	2.1117(7)	2.139	2.141	2.146	2.141(7)	2.141	2.143	2.149
Ta(1)	–P(1)					2.737(4)	2.875	2.812	2.754
Bond	Exptl	$\alpha\text{-P}_4\text{S}_5$			$(\text{TaCl}_5)(\alpha\text{-P}_4\text{S}_5)$				
		B3LYP	BP86	LMP2	Exptl	B3LYP	BP86	LMP2	
P(1)	–P(3)	2.269(1)	2.303	2.308	2.316	2.289(3)	2.314	2.324	2.330
	–S(12)	2.179(1)	2.170	2.176	2.185	2.181(3)	2.180	2.185	2.196
	–S(14)	2.130(1)	2.157	2.159	2.156	2.134(2)	2.151	2.155	2.153
P(2)	–P(3)	2.240(1)	2.290	2.300	2.293	2.241(2)	2.298	2.305	2.300
	–S(1)	1.950(1)	1.933	1.939	1.943	2.003(2)	1.988	1.999	2.003
	–S(12)	2.098(1)	2.150	2.155	2.158	2.086(2)	2.121	2.125	2.126
	–S(24)	2.100(1)	2.158	2.166	2.158	2.089(2)	2.133	2.138	2.127
P(3)	–S(34)	2.080(1)	2.089	2.086	2.097	2.076(2)	2.087	2.086	2.094
P(4)	–S(14)	2.122(1)	2.145	2.149	2.149	2.134(2)	2.144	2.146	2.151
	–S(24)	2.134(1)	2.142	2.142	2.147	2.147(3)	2.157	2.161	2.162
Ta(1)	–S(34)	2.145(1)	2.182	2.195	2.189	2.145(3)	2.174	2.183	2.180
	–S(1)					2.665(2)	2.843	2.779	2.735
Bond	Exptl	$\beta\text{-P}_4\text{S}_5$			$(\text{TaCl}_5)(\beta\text{-P}_4\text{S}_5)$				
		B3LYP	BP86	LMP2	Exptl	B3LYP	BP86	LMP2	
P(1)	–P(3)	2.302(3)	2.346	2.361	2.343	2.304(1)	2.342	2.351	2.328
	–S(12)	2.128(3)	2.144	2.145	2.150	2.092(1)	2.126	2.128	2.123
	–S(14)	2.117(3)	2.144	2.145	2.150	2.090(2)	2.126	2.128	2.123
P(2)	–S(12)	2.122(2)	2.147	2.153	2.152	2.144(2)	2.153	2.160	2.166
	–S(23)	2.122(2)	2.147	2.153	2.152	2.126(2)	2.148	2.153	2.154
	–S(24)	2.134(4)	2.163	2.167	2.164	2.120(2)	2.159	2.162	2.161
P(3)	–S(23)	2.128(3)	2.144	2.145	2.150	2.118(2)	2.142	2.145	2.152
	–S(34)	2.117(3)	2.144	2.145	2.150	2.113(2)	2.142	2.144	2.152
P(4)	–S(14)	2.117(3)	2.147	2.153	2.152	2.131(2)	2.153	2.160	2.166
	–S(24)	2.132(4)	2.163	2.167	2.164	2.116(2)	2.159	2.162	2.161
Ta(1)	–S(34)	2.117(3)	2.147	2.153	2.152	2.115(2)	2.148	2.153	2.154
	–P(1)					2.762(1)	2.895	2.822	2.765
Bond	Exptl ^[b]	$\beta\text{-P}_4\text{S}_6$			$(\text{TaCl}_5)(\beta\text{-P}_4\text{S}_6)$				
		B3LYP	BP86	LMP2	Exptl	B3LYP	BP86	LMP2	
P(1)	–S(1)	1.914(4)	1.930	1.937	1.942	1.990(2)	1.977	1.985	1.992
	–S(12)	2.089(4)	2.142	2.149	2.143	2.074(2)	2.125	2.129	2.124
	–S(13)	2.095(4)	2.142	2.150	2.143	2.104(3)	2.125	2.130	2.123
	–S(14)	2.086(4)	2.136	2.135	2.134	2.080(2)	2.122	2.124	2.117
P(2)	–P(3)	2.309(4)	2.360	2.369	2.362	2.305(3)	2.356	2.365	2.356
	–S(12)	2.110(4)	2.139	2.141	2.147	2.143(2)	2.148	2.150	2.159
	–S(24)	2.123(4)	2.146	2.150	2.150	2.118(3)	2.143	2.147	2.146
P(3)	–S(13)	2.115(4)	2.139	2.141	2.147	2.138(3)	2.146	2.149	2.156
	–S(34)	2.104(4)	2.146	2.150	2.150	2.146(3)	2.142	2.145	2.149
P(4)	–S(14)	2.145(5)	2.188	2.201	2.187	2.159(3)	2.193	2.201	2.192
	–S(24)	2.092(5)	2.135	2.138	2.142	2.098(3)	2.136	2.139	2.144
Ta(1)	–S(34)	2.145(5)	2.135	2.138	2.142	2.121(3)	2.135	2.138	2.141
	–S(1)					2.702(2)	2.912	2.846	2.798

[a] Experimental data taken from Ref. [43]. [b] Experimental data taken from Ref. [8].

bonds P(2)–S(12) and P(4)–S(14) are elongated, P(2)–S(24) again is shortened. $(\text{TaCl}_5)(\alpha\text{-P}_4\text{S}_5)$ and $(\text{TaCl}_5)(\beta\text{-P}_4\text{S}_6)$ show a quite pronounced elongation of the P–S_{terminal} bonds as mentioned earlier. Besides, bonds P(1)–P(3) and P(4)–S(24)

metries on the DFT and local MP2 potential energy hypersurfaces. Structural parameters and the related binding energies (with respect to dissociation of the adducts into their phosphorus sulfide and the TaCl₅ fragments) are compiled

in $(\text{TaCl}_5)(\alpha\text{-P}_4\text{S}_5)$ and P(2)–S(12) and P(3)–S(13) in $(\text{TaCl}_5)(\beta\text{-P}_4\text{S}_6)$ are elongated, bonds P(2)–S(12) in $(\text{TaCl}_5)(\alpha\text{-P}_4\text{S}_5)$ and P(1)–S(12) in $(\text{TaCl}_5)(\beta\text{-P}_4\text{S}_6)$ are shortened. Interestingly, LMP2 and DFT predict very similar changes in these bond lengths, as is evident from Figures 1–4. We conclude that these changes are primarily induced by the weak chemical bond formed between TaCl₅ and the individual cages, which is properly described both by LMP2 and DFT, whereas van der Waals dispersion, even though constituting an important fraction of the overall binding energy, does not induce any significant changes in the intramolecular bonds of the cages.

Alternative coordination

modes: For all phosphorus sulfide cages, only one coordination type was observed experimentally. In contrast, in the $\alpha\text{-P}_4\text{S}_5$, $\beta\text{-P}_4\text{S}_5$, and $\beta\text{-P}_4\text{S}_6$ cages, there are chemically different phosphorus atoms available as possible bonding partners, and all phosphorus sulfide cages could coordinate through sulfur atoms within the cage framework as well. However, phosphorus atoms connected to three sulfur atoms were not found to form a coordinative bond to the metal chlorides under investigation, in contrast to the case of P₄S₃.^[1c,k-o] In fact, coordination through bridging sulfur atoms of the cages could not be observed at all with the metal chlorides used, and only one example for such coordination type is known.^[1k,o]

Alternative coordination sites of the phosphorus sulfides were explored by locating the corresponding minimum energy geo-

Table 2. Binding energies [kJ mol⁻¹] of the structures and their coordination alternatives.

Adduct	Coord. through	Fig. no. ^[a]	B3LYP	BP	LMP2 ^[b]
			<i>E</i> _{bind}	<i>E</i> _{bind}	<i>E</i> _{bind}
(TaCl ₅)(α-P ₄ S ₄)	P	(1)	-8.861	-17.959	-85.914
	S	(2)	+5.638	-1.654	-74.421
(TaCl ₅)(α-P ₄ S ₅)	S(1)	(4)	-5.759	-12.382	-76.191
	S(1)	(1)	-9.224	-16.499	-89.630
	S(14)	(2)	+1.391	-8.031	-85.552
	P(4)	(3)	-1.298	-11.368	-78.624
	S(34)	(5)	+9.195	+1.324	-74.563
	S(1)	(6)	-6.115	-11.964	-73.559
	P(1)	(7)	-3.907	-18.038	-72.159
	P(3)	(8)	+6.326	-3.462	-72.159
(TaCl ₅)(β-P ₄ S ₅)	P(1)	(1)	-9.589	-19.577	-93.096
	S(12)	(2)	+0.166	-9.646	-88.377
	P(2)	(3)	-5.295	-14.952	-86.529
	S(24)	(4)	+2.656	-6.179	-80.043
(TaCl ₅)(β-P ₄ S ₆)	S(1)	(5)	-0.610	-6.154	-75.845
	P(2)	(1)	-6.852	-17.374	-93.644
	S(24)	(2)	+4.483	-5.058	-84.444
	P(4)	(3)	-1.444	-11.854	-82.592
	S(12)	(4)		+3.452	-78.114
	S(1)	(6)	-0.041	-5.485	-74.677
(TaCl ₅) ₂			+1.859	-9.763	-80.974

[a] Numbers are given in Figure 1–4. [b] Ext. domains.

in Figures 1–4 and Tables 1 and 2. Table 3 demonstrates that the deviations between local and canonical MP2 are rather small, especially when extended domains are employed (as in the present work).

The binding between the TaCl₅ subunit and the individual phosphorus sulfide cages is rather delicate and needs some discussion. Comparison of the DFT and local MP2 binding energies in Table 2 reveals that DFT grossly underestimates the binding between the two subunits. In fact, the binding energy predicted by DFT is even substantially smaller than that of a hydrogen bond, occurring, for example, in the water dimer (about 20 kJ mol⁻¹). This is particularly true for the case of the hybrid functional, where self-interaction is reduced owing to admixing of nonlocal (Hartree–Fock) exchange. At the level of Hartree–Fock theory, similar binding energies are obtained as for DFT/B3-LYP. Nevertheless, a weak bond is formed between TaCl₅ and the individual cages at the Hartree–Fock level, which is, for example, reflected by the fact that the localization procedure (used for the subsequent local MP2 treatment; see above) generates a local bicentric orbital involving the Ta and the P (or S) atoms of the related cage (Figure 7). The gain in energy obtained by forming this bond, however, is to a large extent offset by exchange repulsion and geometrical deformation energies. Hence, the net energy gain due to formation of this bond is quite small. Nevertheless, this bond appears to be responsible for the subtle changes of the bond lengths within the individual cages resulting from coordination (see above).

Table 3. Interaction energies [kJ mol⁻¹] calculated with X=T basis set at Hartree–Fock, local (with normal and by one-bond extended domains), and canonical MP2 level of theory.

	Coord. through	Fig. no. ^[a]	HF	LMP2	LMP2 ^[b]	MP2
(TaCl ₅)(α-P ₄ S ₄)	P	(1)	-29.728	-102.514	-107.752	-107.382
	S	(2)	-9.935	-89.782	-97.421	-97.991
(TaCl ₅)(α-P ₄ S ₅)	S(1)	(4)	-53.992	-117.157	-123.589	-123.479
	S(1)	(1)	-50.559	-122.561	-127.951	-127.709
	S(1)	(6)	-48.086	-110.063	-116.378	-116.285
	P(1)	(7)	-19.047	-92.321	-98.138	-97.885
	P(4)	(3)	-12.891	-89.570	-95.903	-95.804
	S(14)	(2)	-11.343	-102.668	-110.258	-110.537
	S(34)	(5)	-1.549	-87.345	-94.692	-95.105
	P(3)	(8)	-4.352	-86.084	-92.486	-92.910
(TaCl ₅)(β-P ₄ S ₅)	P(1)	(1)	-27.659	-106.232	-114.329	-114.996
	P(2)	(3)	-20.223	-99.920	-105.287	-104.749
	S(12)	(2)	-11.868	-104.690	-112.881	-112.927
	S(24)	(4)	-14.758	-97.414	-106.424	-106.665
(TaCl ₅)(β-P ₄ S ₆)	S(1)	(5)	-36.085	-101.883	-106.156	-106.016
	P(2)	(1)	-20.603	-107.319	-113.429	-112.913
	P(4)	(3)	-12.573	-94.615	-100.367	-99.935
	S(12)	(4)	+8.252	-93.683	-101.250	-101.313
	S(24)	(2)	-6.027	-101.071	-108.202	-108.151
	(TaCl ₅) ₂			-169.072	-241.826	-246.380

[a] Numbers are given in Figure 1–4. [b] Ext. domains.

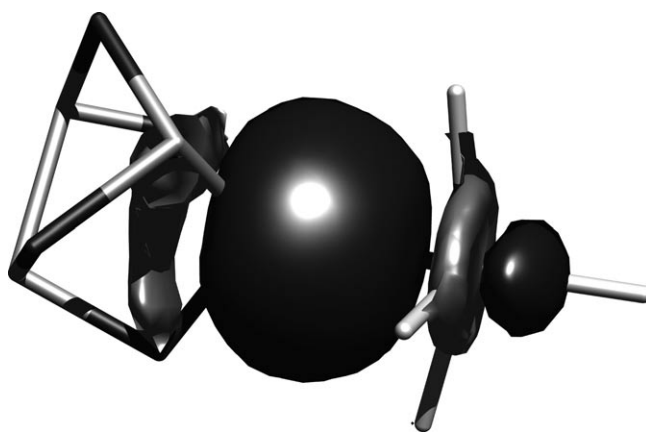


Figure 7. Isoplot of the binding orbital between (TaCl₅) and (α-P₄S₄) fragments of value 0.015. This orbital was obtained by the Pipek–Mezey localization procedure from the set of canonical Hartree–Fock orbitals.

At the MP2 level, however, substantially larger binding energies are obtained (76–93 kJ mol⁻¹). This difference could be attributed to long-range dispersion electron correlation effects (such as van der Waals forces), which are absent both at the Hartree–Fock level and in DFT (with presently available exchange–correlation functionals), but which are accounted for at the level of MP2. Considering

the large polarizabilities of the individual subunits, noticeable van der Waals contributions to the binding energy are not too surprising. Taking into account the astonishingly small DFT binding energies, one may even argue that the major contributions to the binding energies of the individual adducts are actually indeed of van der Waals type. Van der Waals type interactions between closed-shell subunits are ubiquitous in inorganic chemistry (see Ref. [44] for a review). For example, they are clearly dominant in the aurophilic attraction between Au^I ions.^[45] For a definite answer about the role of van der Waals forces in the adducts characterized in the present work, however, a more detailed study of the interactions between the phosphorus sulfide and the TaCl₅ subunits is required (e.g., based on a partitioning of the LMP2 correlation energy), as was done previously for dimers of coinage metal complexes.^[45]

In any case, because of the poor description of the binding of the adducts by DFT, we will focus in the following discussion on the results obtained at the level of local MP2. In Figures 1–4, the different adduct isomers are enumerated in descending order with respect to their binding energies. For (TaCl₅)(α -P₄S₄) the alternative coordination mode (2) through a sulfur atom is 11.49 kJ mol⁻¹ less stable than the observed coordination through phosphorus.

For (TaCl₅)(β -P₄S₅), the observed coordination through one of the phosphorus dumbbell atoms leads to the adduct with lowest energy. Coordination mode 2 through one of the four equivalent sulfur atoms and coordination mode 3 through an isolated phosphorus atom are 4.72 kJ mol⁻¹ and 6.57 kJ mol⁻¹, respectively, less stable. The binding energies of adducts coordinated through the sulfur bridge (4) decrease even further (by 13.05 kJ mol⁻¹) relative to the global minimum.

For (TaCl₅)(α -P₄S₅), the coordination mode (4) through the terminal sulfur atom, observed in the conformation in the crystal, is according to the LMP2 calculations 13.44 kJ mol⁻¹ above the global minimum, conformation 1, obtained from 4 by rotation about the P–S_{terminal} axis. As already stated, this rotation is not sterically hindered and requires only a small activation energy. The alternative—and most stable—conformer therefore is possibly not realized in the crystal for packing reasons but may also be the preferred one for the α -P₄S₅ adduct in solution. Coordination mode 2 through the sulfur atom S(14) is still energetically favored relative to 4 by 9.36 kJ mol⁻¹, and even the coordination through the apical phosphorus atom P(4), variant 3, is more stable (by 2.43 kJ mol⁻¹) than the observed conformer. However, the coordination alternatives given as variants 5, 6, 7, and 8 (i.e., isomers coordinated through S(34), another conformational variant to the S(1) linkage) and coordination through the basal phosphorus atoms P(1) or P(3) are energetically less favored (by 1.63, 2.63, 4.03, and 4.03 kJ mol⁻¹, respectively). Notably, the three coordination modes through the terminal sulfur atom feature stronger binding at the (uncorrelated) Hartree–Fock level by about 20 kJ mol⁻¹ relative to the remaining conformers. This result indicates that for such coordination modes, the covalent

bond and eventually also electrostatic interactions play a more pronounced role in the binding than for the remaining conformers.

Finally, the global minimum for (TaCl₅)(β -P₄S₆) features coordination through one of the phosphorus dumbbell atoms P(2) or P(3) (variant 1). The binding energy is 17.80 kJ mol⁻¹ larger than for the experimentally observed coordination through the terminal sulfur atom (variant 5). For this adduct there is a significant mismatch between the structural arrangements occurring in the crystal on the one hand and that of the isolated adduct predicted by theory on the other. Also, other adduct isomers coordinated through the sulfur atom S(24) (variant 2), the apical phosphorus atom P(4) (variant 3), or the sulfur atom S(12) (variant 4), are energetically more stable by 8.60, 6.75, and 2.27 kJ mol⁻¹, respectively, relative to the β -P₄S₆ adduct observed experimentally. However, the alternative conformer for the linkage through the terminal sulfur atom given as variant 6 has a lower binding energy (1.17 kJ mol⁻¹) and is therefore less stable than the conformer observed.

Geometry optimizations for all possible coordination conformers were performed. Other coordination alternatives not listed here were found to be even less stable. Considering the LMP2 dissociation energy of (TaCl₅)₂, which amounts to 80.97 kJ mol⁻¹, the formation of all considered species presented herein is exothermic in the gas phase.

In conclusion, there is a general preference for coordination through basal/dumbbell phosphorus atoms or terminal sulfur atoms (if present). Structural arrangements corresponding to such coordination modes are found to be most stable. A substantial part of the binding energy between the phosphorus sulfide cage and the TaCl₅ subunit can be ascribed to van der Waals dispersion. There is a mismatch between experimental results and theory for one case, where the experimentally found geometry does not correspond to the theoretically predicted global minimum. The existence of a structure corresponding to the global minimum cannot yet be ruled out, particularly as the differences in binding energy for the several adduct isomers are rather small.

Conclusions

Not only the smallest phosphorus sulfide cage molecule P₄S₃^[1] but also cage-like phosphorus sulfides with higher sulfur content can act as ligands in metal complexes. Adducts of α -P₄S₄, β -P₄S₄, α -P₄S₅, β -P₄S₅, β -P₄S₆, and monomeric TaCl₅ or NbCl₅ units could be obtained so far. Phosphorus or sulfur atoms of the sulfide cages in principle can be connected to Lewis acids. We found that the coordination to the cage molecule is favored either to phosphorus sites with one adjacent phosphorus atom or to terminal sulfur sites. Coordination to bridging sulfur sites or to phosphorus sites bound to three sulfur atoms was energetically less stable.

The cage constitution is not changed upon coordination; however, certain bond lengths within the cages change as a result of coordination to the metal.

Generally, bonds between phosphorus atoms and the coordinated terminal sulfur site lengthen considerably. However, bonds involving phosphorus, either directly coordinated or adjacent to a coordinated terminal sulfur site, shorten. The next nearest bonds then lengthen. These relative changes of the individual bond lengths within the cages are rather well described by both DFT and LMP2, which suggests that they are primarily caused by the weak coordinative bond formed between the metal center and the cage. However, the contribution of this bond to the overall binding energy of the adduct is small, and the dominant component appears to be long-range van der Waals dispersion. The latter is not captured by DFT (in conjunction with the usual functionals), which consequently leads to much too small binding energies and too large lengths of the coordinative bond as predicted by this method. MP2, on the other hand, describes van der Waals dispersion at a level corresponding to the uncoupled Hartree–Fock representation of the underlying dynamical polarizabilities (which usually leads to significant overestimation of binding energy in complexes such as the benzene dimer or argon clusters). So, although not highly accurate, MP2 certainly paints a much more realistic picture of the energetics than DFT in a situation in which long-range van der Waals dispersion is of importance (of course, we were lucky that near degeneracy effects were absent in the present system; otherwise, perturbation theory based on a single reference would not be applicable). Hence, we are sure to describe the present system at least qualitatively correct. To further improve the accuracy, coupled cluster calculations with reasonably large basis sets must be performed, which is beyond the scope of the present study. DFT, however, qualitatively fails for the present systems with weak coordinative bonds.

Experimental Section

Synthesis: Only a small number of the phosphorus sulfides P_4S_3 to P_4S_{10} can be obtained by “classical” solid-state synthesis by annealing phosphorus and sulfur: namely, P_4S_3 , α - P_4S_7 , and P_4S_{10} . These sulfides show congruent melting upon heating,^[5] whereas most phosphorus sulfides decompose at higher temperatures or even when stored in solution at room temperature. Thus, the preparation of these phosphorus sulfides has to start from P_4S_3 , α - P_4S_7 , P_4S_{10} , or related compounds such as iodides. In principle, sulfur-rich cages can be desulfurized, for example, with Ph_3P , or sulfur can be added to sulfur-deficient cages using various reagents with weakly bound sulfur, such as Ph_3AsS .^[6]

(TaCl₅)(α -P₄S₅) and (TaCl₅)(β -P₄S₆): Mixtures of phosphorus sulfides were used to examine the reactivity towards the metal halides in a first screening. Phosphorus and sulfur were weighed into fused silica ampoules in different ratios (for example, P:S=4:4 or 4:5). The evacuated ampoules were heated to 330 °C for 2 days and then cooled to room temperature. The resulting brittle yellow mass was ground and used without further purification. As stated in the literature, phosphorus sulfide melts can contain different types of cages, which can exchange sulfur atoms to form an equilibrium distribution of sulfides. Starting from a phosphorus to sulfur ratio of 4:4, 18–62 mol% P_4S_3 , 1–3 mol% α - P_4S_4 , ca. 2 mol% β - P_4S_4 , 19–30 mol% α - P_4S_5 , 10–46 mol% β - P_4S_6 , and 3–7 mol% α - P_4S_7 was found. The composition changed to 14–29 mol% P_4S_3 , 1–2 mol% α - P_4S_4 , 28–39 mol% α - P_4S_5 , 24–27 mol% β - P_4S_6 , and 3–33 mol% α - P_4S_7 upon increasing the sulfur content to a 4:5 ratio.^[7,8]

The phosphorus sulfide mixtures (ca. 90 mg), Ta₂Cl₁₀ (130–140 mg; 0.18–0.20 mmol), and CS₂ (ca. 2 mL) were added to Schlenk flasks and covered with *n*-hexane (1.5 mL) under inert conditions.^[2] After several weeks at room temperature, the liquid phases were removed. Besides greenish-yellow columnar crystals of (TaCl₅)₂(β -P₄S₄), isotypic to (NbCl₅)₂(β -P₄S₄),^[2] a few light yellow plate-like crystals of (TaCl₅)(α -P₄S₅) and (TaCl₅)(β -P₄S₆) could be separated from the residue and dried in an argon stream. (TaCl₅)(α -P₄S₅) could also be obtained from α -P₄S₅ (prepared from P₄S₃ and sulfur in CS₂ according to Refs. [5, 9, 10]) and Ta₂Cl₁₀ or directly from P₄S₃, sulfur, and Ta₂Cl₁₀. (TaCl₅)(β -P₄S₆) could similarly be obtained from P₄S₃, sulfur, and Ta₂Cl₁₀ by employing an excess of sulfur.

Other than (NbCl₅)₂(β -P₄S₄), no further compounds isostructural with niobium pentachloride were found. It is possible that the distinct reduction of niobium(V) to niobium(IV)—owing to the lower redox potential of niobium relative to tantalum—leads to increased formation of chlorinated phosphorus or phosphorus sulfide species.

(TaCl₅)(α -P₄S₄): α -P₄S₄ was prepared as described in Ref. [11]. P₄S₃ (Riedel-de Haën, 55.8%) was purified in boiling water and recrystallized from CS₂.^[10] Then, α -P₄S₃I₂ was prepared from P₄S₃ and iodine by heating the mixture for 2 days at 170 °C.^[12] After recrystallization from CS₂, α -P₄S₃I₂ and [(CH₃)₃Sn]₂S (prepared according to Ref. [13] from (CH₃)₃SnCl and Na₂S·XH₂O in ethanol) in an approximate ratio of 1:1.5 were stirred in CS₂ for 5 days. The product formation was monitored by NMR spectroscopy. A yellow precipitate (α -P₄S₄) formed on cooling and was filtered, washed with dry diethyl ether, and dried. α -P₄S₄ (ca. 50 mg; 0.2 mmol) and Ta₂Cl₁₀ (ca. 100 mg; 0.14 mmol) were covered with CS₂ (2 mL) and *n*-hexane (1.5 mL) in a Schlenk flask. Small orange crystals of (TaCl₅)(α -P₄S₄) formed within a few days.

(NbCl₅)(β -P₄S₅) and (TaCl₅)(β -P₄S₅): α -P₄S₇ was synthesized from P₄S₃ and sulfur (Alfa Aesar, 99.9995%) by annealing the mixture at 330 °C for several days followed by slow cooling to room temperature. In a second step, α -P₄S₇ and triphenylphosphane Ph₃P (Merck, for synthesis, >99%) in a molar ratio of 1:2 were heated at reflux in CS₂ for 1 week in an argon atmosphere. Afterwards, the solvent was removed in an argon stream, and the residue was washed with small portions of cold CHCl₃ to extract Ph₃PS, filtered, and dried. The purity of the thus formed β -P₄S₅ was verified by powder X-ray diffraction. β -P₄S₅ (ca. 210 mg; 0.74 mmol) and Nb₂Cl₁₀ (200 mg; 0.37 mmol) or Ta₂Cl₁₀ (265 mg; 0.37 mmol) were filled into Schlenk flasks. Then, CS₂ (2 mL) and *n*-hexane (1.5 mL) were added. After 2 days, dark red columnar or plate-like crystals of (NbCl₅)(β -P₄S₅) and yellow columnar crystals of (TaCl₅)(β -P₄S₅) were obtained.

All adducts are moisture sensitive and therefore must be handled under inert conditions.

Crystal structure determination: Suitable crystals of the adduct compounds were used for single-crystal X-ray structure analysis. The diffraction data were collected on an imaging plate diffraction system IPDS-I (Stoe) at about 20 °C. Numerical absorption corrections based on crystal descriptions were applied.^[14,15] The structures were solved by direct methods and refined against F_o^2 with the SHELX-97 program package.^[16] All atoms were refined using anisotropic displacement parameters. Details of the crystal structure investigations are available from the Fachinformationszentrum Karlsruhe, D-76344 Eggenstein-Leopoldshafen, Germany (Fax: (+49) 7247-808-666, e-mail: crysdata@fiz-karlsruhe.de) referring to numbers CSD-419157 (TaCl₅)(α -P₄S₄), CDS-419156 (TaCl₅)(α -P₄S₅), CSD-419155 (TaCl₅)(β -P₄S₅), CSD-419165 (NbCl₅)(β -P₄S₅), CSD-419154 (TaCl₅)(β -P₄S₆), the name of the authors, and a citation of the paper.

Computational methods: Minimum energy geometries and relative energies of different isomers of the individual compounds were calculated by employing DFT, as well as second-order Møller–Plesset perturbation theory. For the DFT calculations, the Becke–Perdew BP86^[35] and the B3-LYP^[34] exchange correlation functionals were used. The MP2 calculations were performed because van der Waals forces, which are not included in a DFT treatment with present functionals, are likely to play a significant role in the bonding between the cage and the TaCl₅ subunits. Initial complete active space self-consistent field test calculations, also performed in the context of this work, indicate that a multireference treatment is not

required for a proper description of the binding between the TaCl₅ subunit and the individual cages.

For the MP2 calculations, the local MP2 method^[17,19] as implemented in the MOLPRO^[18] program package was used. The density fitting (DF) approximation for the electron repulsion integrals was invoked, which allows for much more efficient algorithms to be used (in particular also for computing analytic energy gradients^[20] as required for geometry optimizations) at virtually no loss in accuracy.

It was demonstrated previously that local correlation methods avoid basis set superposition error (BSSE) effects to large extent by construction.^[21] Hence, as a further bonus of local MP2, quasi-BSSE-free geometry optimizations can be carried out in a convenient way, that is, without any need for counterpoise correction^[31] of the individual energy gradients involved.

For the tantalum atoms, the Stuttgart/Cologne ECP60MWB quasi-relativistic energy-adjusted pseudopotential, which substitutes the Ta¹³⁺ core orbitals, together with the related (8s7p6d2f1g)/[6s5p3d2f1g] AO basis set was employed.^[22,23] For the remaining atoms, the augmented correlation consistent AO basis sets aug-cc-pVXZ of Dunning^[24,25] were used (X=D for geometry optimizations, X=T for single-point energies). As fitting basis sets for the DF approximation, the auxiliary basis related to the aug-cc-pVXZ AO sets optimized for DF-MP2^[26] were taken for the MP2 component of energy and gradient, while for the Hartree-Fock part the JK fitting basis sets of Weigend^[27] related to the cc-pV(X+1)Z AO basis were used. For the tantalum/ECP60MWB AO basis no optimized fitting basis set is yet available. Therefore, the fitting basis set related to the QZVPP AO basis^[28] was used, which should be sufficiently large to guarantee accurate fitting of the individual orbital product densities.

The localized molecular orbitals spanning the occupied orbital space of the Hartree-Fock reference were generated by using the Pipek-Mezey localization procedure.^[29] Pair domains were constructed by using a completeness criterion^[30] of 0.98 and 0.985 for the X=D and X=T AO basis sets, respectively. For all calculations the pair domains were further extended by all next nearest-neighbor centers.

For the DFT calculations (carried out by utilizing the TURBOMOLE program package^[33,36]), the same AO and auxiliary basis sets and the same pseudopotential as for the local MP2 calculations were used. For both geometry optimizations and single-point energy calculations X=T was used. The final interaction energies, obtained at DFT and MP2 levels, were all counterpoise-corrected (in the case of local MP2 to remove the BSSE of the Hartree-Fock energy) and also include the relaxation energies of the individual fragments.^[32]

Acknowledgements

We thank Manuele Avola for experimental help, and H. C. Starck for the generous gift of Nb₂Cl₁₀ and Ta₂Cl₁₀. Financial support from the Deutsche Forschungsgemeinschaft (DFG) is gratefully acknowledged.

- [1] a) J. G. Riess, J. R. Van Wazer, *J. Am. Chem. Soc.* **1966**, *88*, 2166; b) P. J. Ashley, E. G. Torrible, *Can. J. Chem.* **1969**, *47*, 2587; c) A. W. Cordes, R. D. Joyner, R. D. Shores, E. D. Dill, *Inorg. Chem.* **1974**, *13*, 132; d) M. L. Walker, J. L. Mills, *Inorg. Chem.* **1975**, *14*, 2438; e) G. G. Alange, A. J. Banister, *J. Inorg. Nucl. Chem.* **1978**, *40*, 203; f) M. Di Vaira, M. Peruzzini, P. Stoppioni, *J. Chem. Soc. Chem. Commun.* **1983**, 903; g) M. Di Vaira, M. Peruzzini, P. Stoppioni, *J. Chem. Soc. Dalton Trans.* **1985**, 291; h) U. Thewaldt, K. Holl, *Z. Naturforsch. B* **1988**, *43*, 467; i) J. Wachter, *Angew. Chem.* **1998**, *110*, 782; *Angew. Chem. Int. Ed.* **1998**, *37*, 750; j) C. Aubauer, E. Irran, T. M. Klapötke, W. Schnick, A. Schulz, J. Senker, *Inorg. Chem.* **2001**, *40*, 4956; k) A. Adolf, M. Gonsior, I. Krossing, *J. Am. Chem. Soc.* **2002**, *124*, 7111; l) E. Guidoboni, I. de Los Rios, A. Ienco, L. Marvelli, C. Maelli, A. Romerosa, R. Rossi, M. Peruzzini, *Inorg. Chem.* **2002**, *41*, 659; m) I. de Los Rios, F. Mani, M. Peruzzini, P.

- Stoppioni, *J. Organomet. Chem.* **2004**, *689*, 164; n) M. Di Vaira, I. de Los Rios, F. Mani, M. Peruzzini, P. Stoppioni, *Eur. J. Inorg. Chem.* **2004**, 293; o) I. Raabe, S. Antonijevic, I. Krossing, *Chem. Eur. J.* **2007**, *13*, 7510.
- [2] H. Nowotnick, K. Stumpf, R. Blachnik, H. Reuter, *Z. Anorg. Allg. Chem.* **1999**, *625*, 693.
- [3] A. Pfitzner, D. Hoppe, *Z. Anorg. Allg. Chem.* **2006**, *632*, 1771.
- [4] D. Hoppe, A. Pfitzner, *Z. Naturforsch. B* **2009**, *64*, 58.
- [5] R. Blachnik, A. Hoppe, *Z. Anorg. Allg. Chem.* **1979**, *457*, 91.
- [6] M. E. Jason, *Inorg. Chem.* **1997**, *36*, 2641.
- [7] T. Bjorholm, H. J. Jacobsen, *J. Am. Chem. Soc.* **1991**, *113*, 27.
- [8] R. Blachnik, U. Peukert, A. Czediwoda, B. Engelen, K. Boldt, *Z. Anorg. Allg. Chem.* **1995**, *621*, 1637.
- [9] G. Brauer, *Handbuch der präparativen Anorganischen Chemie*, Vol. 1, Enke, Stuttgart, **1975**.
- [10] S. van Houten, E. H. Wiebenga, *Acta Crystallogr.* **1957**, *10*, 156.
- [11] a) W. Bues, M. Somer, W. Brockner, *Z. Naturforsch. A* **1981**, *36*, 842; b) A. M. Griffin, P. C. Minshall, G. M. Sheldrick, *J. Chem. Soc. Chem. Commun.* **1976**, 809.
- [12] R. Blachnik, G. Kurz, U. Wickel, *Z. Naturforsch. B* **1984**, *39*, 778.
- [13] M. Gingras, T. H. Chan, D. N. Harpp, *J. Org. Chem.* **1990**, *55*, 2078.
- [14] X-RED 1.26, Program for data reduction, STOE & Cie, Darmstadt, Germany, **2004**.
- [15] X-SHAPE 2.05, Program for crystal optimization for numerical absorption correction, STOE & Cie, Darmstadt, Germany, **2004**.
- [16] G. M. Sheldrick, SHELX-97, Program for crystal structure determination, University of Göttingen, Germany, **1997**.
- [17] M. Schütz, G. Hetzer, H.-J. Werner, *J. Chem. Phys.* **1999**, *111*, 5691.
- [18] H.-J. Werner, P. J. Knowles, R. Lindh, F. R. Manby, M. Schütz, and others, MOLPRO, Version 2008.1, a package of ab initio programs; see <http://www.molpro.net>.
- [19] H.-J. Werner, F. R. Manby, P. J. Knowles, *J. Chem. Phys.* **2003**, *118*, 8149.
- [20] M. Schütz, H.-J. Werner, R. Lindh, F. M. Manby, *J. Chem. Phys.* **2004**, *121*, 737.
- [21] M. Schütz, G. Rauhut, H.-J. Werner, *J. Phys. Chem. A* **1998**, *102*, 5997.
- [22] D. Andrae, U. Haeussermann, M. Dolg, H. Stoll, H. Preuss, *Theor. Chim. Acta* **1990**, *77*, 123.
- [23] J. M. L. Martin, A. Sundermann, *J. Chem. Phys.* **2001**, *114*, 3408.
- [24] "Gaussian Basis Sets for Molecular Calculations, chapter 1 in Methods of electronic structure theory" T. H. Dunning, Jr., P. J. Hay in *Modern theoretical chemistry*, Vol. 3 (Ed.: H. F. Schaefer), Plenum Press, New York, **1977**, pp. 1–27.
- [25] R. A. Kendall, T. H. Dunning, Jr., R. J. Harrison, *J. Chem. Phys.* **1992**, *96*, 6796.
- [26] F. Weigend, A. Köhn, C. Hättig, *J. Chem. Phys.* **2002**, *116*, 3175.
- [27] F. Weigend, *Phys. Chem. Chem. Phys.* **2002**, *4*, 4285.
- [28] A. Hellweg, C. Hättig, S. Höfener, W. Klopper, *Theor. Chem. Acc.* **2007**, *117*, 587.
- [29] J. Pipek, P. Mezey, *J. Chem. Phys.* **1989**, *90*, 4916.
- [30] J. W. Boughton, P. Pulay, *J. Comput. Chem.* **1992**, *13*, 736.
- [31] S. F. Boys, F. Bernardi, *Mol. Phys.* **1970**, *19*, 553.
- [32] J. Stålring, M. Schütz, R. Lindh, G. Karlström, P.-O. Widmark, *Mol. Phys.* **2002**, *100*, 3389.
- [33] a) K. Eichkorn, O. Treutler, H. Öhm, M. Häser, R. Ahlrichs, *Chem. Phys. Lett.* **1995**, *240*, 283; b) K. Eichkorn, F. Weigend, O. Treutler, R. Ahlrichs, *Theor. Chem. Acc.* **1997**, *97*, 119.
- [34] A. D. Becke, *J. Chem. Phys.* **1993**, *98*, 5648.
- [35] J. P. Perdew, *Phys. Rev. B* **1986**, *33*, 8822.
- [36] Electronic Structure Calculations on Workstation Computers: The Program System TURBOMOLE. R. Ahlrichs, M. Bär, M. Häser, H. Horn, C. Kölmel, *Chem. Phys. Lett.* **1989**, *162*, 165.
- [37] M. Kunz, I. D. Brown, *J. Solid State Chem.* **1995**, *115*, 395.
- [38] H. Henke, *Z. Kristallogr.* **1992**, *198*, 1.
- [39] D. Neubauer, J. Weiss, *Z. Anorg. Allg. Chem.* **1960**, *303*, 28.
- [40] R. Steudel, T. Sandow, J. Steidel, *J. Chem. Soc. Chem. Commun.* **1980**, 180.
- [41] D. Clark, *J. Chem. Soc.* **1952**, 1615.

- [42] P. Luger, H. Bradaczek, R. Steudel, M. Rebsch, *Chem. Ber.* **1976**, *109*, 180.
- [43] C. C. Chang, R. C. Haltiwanger, A. D. Norman, *Inorg. Chem.* **1978**, *17*, 2056.
- [44] P. Pyykkö, *Chem. Rev.* **1997**, *97*, 597.
- [45] a) N. Runeberg, M. Schütz, H.-J. Werner, *J. Chem. Phys.* **1999**, *110*, 7210; b) L. Magnko, M. Schweizer, G. Rauhut, M. Schütz, H. Stoll, H.-J. Werner, *Phys. Chem. Chem. Phys.* **2002**, *4*, 1006.

Received: February 10, 2009
Published online: June 16, 2009